
Generalized Permutation Framework for Testing Model Variable Significance

Yue Wu
yueswu@uw.edu

Kenji Nakamichi

Russell Van Gelder

Aaron Lee

Abstract

A common problem in machine learning is determining if a variable significantly contributes to a model's prediction performance. This problem is aggravated for datasets, such as gene expression datasets, that suffer the worst case of dimensionality: a low number of observations along with a high number of possible explanatory variables. In such scenarios, traditional methods for testing variable statistical significance or constructing variable confidence intervals may not apply. To address these problems, we developed a novel generalized permutation framework (GPF) for testing the significance of variables in supervised models. Our permutation framework has three main advantages. First, it is non-parametric and does not rely on distributional assumptions or asymptotic results. Second, it is model agnostic and allows one to construct the null distribution for any metric of interest for a feature in a supervised model. Third, it can overcome co-linearity in high dimensional datasets and determine contribution of each variable. We demonstrate the performance of the generalized permutation framework on synthetic datasets versus existing methods, and then applied it to multi-class classification of brain regions in RNA expression data, and used this framework to show variable-level statistical significance and interactions.

1 Introduction

The curse of dimensionality has often posed challenges to machine learning, not only in terms of training a model, but also for understanding the trained model. It is often as important to be able to interpret a fitted model. For example, an interpretable model on gene-expression data should allow one to validate the model predictions externally using independent molecular assays and gain insight into diseases. Furthermore, a model would be quantifiably interpretable if it identified the relative contributions of different genes to modeling and predicting disease, thereby helping researchers prioritize the molecular assays.

Classically, the significance of variable contributions to models are measured by p-values. For example, in generalized linear models the contribution of each explanatory variable can be quantified by their p-values or 95% confidence intervals. More generally, non-linear models, such as random forests and deep learning based models, have achieved success in modeling and predicting labeled targets in a supervised setting, but are less easily interpretable. Frameworks have been proposed for interpreting these models, such as tree feature importance [6], gradient based attention and saliency maps [32, 34] or game theoretic interpretations such as SHAP [24]. One of the key shortcomings of these frameworks is the lack of traditional statistical measures for the explanatory variables.

In this paper, we present a novel generalized permutation framework (GPF) that provides traditional statistical measures such p-values and confidence intervals for explanatory variables in non-linear

models. Our three main contributions are: First, the GPF allows one to construct the null distribution for the contribution of any feature in a supervised model for any metric of interest. Second, the GPF makes no distributional nor conditional assumptions about the explanatory variables or target variable. Third, the GPF can overcome co-linearity problems in high dimensional datasets by applying permutations to subsamples of the variables. The GPF was first demonstrated and compared to state-of-the-art models on synthetic datasets. Then it was applied to a real-world RNA expression dataset, which suffer from the curse of dimensionality, where it was able to discover the genes that make significant contributions in classifying brain regions.

2 Review of related work

2.1 Model explainers

In the case of complex models that allow convoluted interactions between variables, such as XGBoost [8] and Deep Neural Networks [14], there has been extensive research into frameworks that explain the model predictions. Model explainers such as LIME [29] and SHAP [24] show the impact each observation $\{x_{mj}\}_{j=1}^P$, where P is the number of variables, in making prediction \hat{y}_m . They can also measure the overall impact of each variable $x_{.j}$ by combining the impact of each observation $\{x_{ij}\}_{i=1}^N$. Kumar et al. [17] showed that mathematical problems arise when SHAP is used for feature importance in tree models. Furthermore, SHAP does not provide a confidence interval on the impact of each variable in the model.

2.2 Randomization tests

Model-X knockoffs and Conditional Randomization Test (CRT) were proposed together in [7]. The CRT algorithm is reproduced in Algorithm A1. CRT’s feature importance statistic $T_j(\mathbf{X}, \mathbf{y})$ was chosen to be the Lasso coefficient difference (LCD) statistic, as the authors focused on linear Gaussian models. Moreover, CRT can be applied to non-linear models if the feature importance statistic is chosen to be model appropriate. However, CRT suffers a major shortcoming, as it requires knowledge of the conditional distribution to sample knockoffs (Algorithm A1 Eq. 6). The conditional and thereby marginal distributions of the variables, $\mathcal{F}(\mathbf{X})$, is only known if the variables were chosen in designed experiments. In general for most datasets, one needs to learn the joint distribution of the variables \mathbf{X} and the response \mathbf{y} , as well as marginal distribution of the variables, $\mathcal{F}(\mathbf{X})$. Therefore the $\mathcal{F}(\mathbf{X})$ requirement limits the usefulness of CRT.

Another area of concern was CRT’s computational costs, as it involved re-training each of the $P \times R$ simulated design matrices against the response. Model-X knockoffs was presented as a computationally optimized version of CRT for linear Gaussian models, where all the knockoffs $\mathbf{X}_j^{(r)}$ are generated at once for all $j = 1, \dots, P$, and these knockoffs appended to the original \mathbf{X} to create a new design matrix \mathbf{X}' that is $N \times 2P$. Then Lasso is fit on \mathbf{X}' , with the intuition that the coefficients for the knockoffs $X_j^{(r)}$ as well as those variables X_j that are independent of the response \mathbf{y} will shrink to 0. However, the authors themselves showed that CRT had higher power than model-X knockoffs.

The Holdout Randomization Test (HRT) [36] is a specialized CRT that avoids re-training by splitting the dataset into training and test datasets. HRT fits the model on the training dataset, and evaluates on conditionally sampled test data, which again requires knowledge of the marginal distribution, $\mathcal{F}(\mathbf{X})$. Philosophically, HRT is similar to SHAP as they measure the conditional mutual information between the variables and the response.

An alternate method is the Conditional Permutation Test (CPT) [4], which uses permutations based on ordered statistics to perturb the $\mathbf{X}_{\mathbf{p}p=1, \dots, P}$ variables. The ordered statistics still require approximations of the conditional distribution $\mathcal{F}(\mathbf{X}_j | \{\mathbf{X}_{\mathbf{p}}\}_{p \neq j})$.

CRT, HRT and CPT all require some knowledge of the conditional distribution $\mathcal{F}(\mathbf{X}_j | \{\mathbf{X}_{\mathbf{p}}\}_{p \neq j})$, which is not always available. Furthermore, computation gains in HRT might indirectly obfuscate the ability of the statistical model used to overfit the training data.

2.3 Permutation tests

An alternative to conditional randomization, which requires conditional knowledge about the variables, is to use permutations. A standard technique to construct the null distribution is by using the permutation plug-in estimate [31, 38, 15, 11, 13]. In the permutation plug-in technique, the null distribution for a statistic of interest is constructed by randomly permuting the labels, and then computing the statistic for the permuted label data and unpermuted covariates. The intuition is that if the labels are scrambled, the relationship between the labels and the variable will be broken, and no variable should be able to reliably predict the scrambled labels. Thus the statistic computed on the scrambled labels is a distribution of the statistic when the null hypothesis is true.

Li and Tibshirani [21] applied the permutation plug-in estimate to construct the null distributions of the resampled rank statistic of genes for classifying genetic conditions. Their algorithm, SAMseq, is summarized in Algorithm A4. Genes that are differentially expressed can then be tested against their null distributions in a non-parametric way without relying on distributional assumptions as in the popular DESeq2 method [23]. Label permutation has also been applied to evaluate model predictive performance in [12, 40, 2], and to test model variable selection techniques on chemical compound data in [22]. Additionally, Strobl et al. [35] permuted the variables in synthetic data to study how correlated variables affected the construction of trees in Random Forests. In contrast, we use permutations in a model-independent fashion to analyze statistical contributions of each variable.

3 Generalized Permutation Framework (GPF)

In this paper, we extend the permutation plug-in estimate to construct null distributions for supervised models generally, and are not constrained to specific model types. To do this, we propose the construction of two types of null distributions by using permutations on different inputs of the supervised model. Let $\Phi(\cdot)$ be a permutation function that randomly permutes an input vector. The two types of permutations can be expressed as:

1. Permute labels \mathbf{y} : $\Phi_y(\cdot) = \Phi(\mathbf{y})$.
2. Permute a variable $\mathbf{x}_{\cdot,j} = \{x_{ij}\}_{i=1}^N$, but leave \mathbf{y} and $\{\mathbf{x}_{\cdot,k}\}_{k \neq j}$ unchanged: $\Phi_x(\cdot) = \Phi(\mathbf{x}_{\cdot,j})$.

3.1 Subset-GPF

A naive implementation of the generalized permutation framework (Naive-GPF) incorporates these permutations and is shown in Algorithm A2. Naive-GPF is as computationally as expensive as CRT. Therefore we take a subset approach and introduce Subset-GPF in Algorithm 1. The intuition of

Algorithm 1 Subset-GPF

- 1: **Input:** labels $\mathbf{y} = \{y_i\}_{i=1}^N$, covariates $\mathbf{X} = \{x_{ij}\}_{i=1,j=1}^{N,P}$, and supervised model f
 - 2: **hyperparameters:** subsample size K , M variable indices of interest, $\{j_m \in \{1, \dots, P\}\}_{m=1}^M$ for the corresponding variables $\{\mathbf{x}_{\cdot,j_m}\}_{m=1}^M$
 - 3: **for** $m = 1$ **to** M **do**
 - 4: **for** $r = 1$ **to** R **do**
 - 5: Sample $K - 1$ times without replacement from $\{1, \dots, P\} \setminus j_m$ to get $\{k'\}$
 - 6: Let $\mathbf{X}_{sub} = \{\mathbf{x}_{\cdot,k}\}_{k \in \{k'\}}$
 - 7: Concatenate \mathbf{x}_{\cdot,j_m} with \mathbf{X}_{sub} to obtain \mathbf{Z} with dimensions $N \times K$
 - 8: Split \mathbf{y} and \mathbf{Z} into training and test sets.
 - 9: Train and compute the test statistic $T_{j_m}^{(r)}$ from \mathbf{y} , \mathbf{Z} and f .
 - 10: Permute the variable of interest, $\mathbf{x}'_{\cdot,j_m} = \Phi_x(\mathbf{x}_{\cdot,j_m})$
 - 11: Concatenate \mathbf{x}'_{\cdot,j_m} with \mathbf{X}_{sub} to obtain \mathbf{Z}'
 - 12: Train and compute test statistic $T_{j_m}'^{(r)}$ from \mathbf{y} , \mathbf{Z}' and f using same train/test split.
 - 13: **end for**
 - 14: **end for**
 - 15: **Output:** $\{\{T_{j_m}^{(r)}\}_{r=1}^R\}_{m=1}^M$ and $\{\{T_{j_m}'^{(r)}\}_{r=1}^R\}_{m=1}^M$
-

Table 1: Framework Comparison

Framework	Dataset	Perturbation	Re-train f	H_0	Test Stat
SHAP	Train Test	exclude(X_j)	No	$X_j \perp\!\!\!\perp Y f, \{X_p\}_{p \neq j}$	Model score
Perm. Importance	Train Test	$\Phi(X_j)$	No	$X_j \perp\!\!\!\perp Y f, \{X_p\}_{p \neq j}$	Model score
HRT	Test	$\mathcal{F}(X_j \{X_p\}_{p \neq j})$	No	$X_j \perp\!\!\!\perp Y f, \{X_p\}_{p \neq j}$	Model score
HRT-CV	Test	$\mathcal{F}(X_j \{X_p\}_{p \neq j})$	CV	$X_j \perp\!\!\!\perp Y f, \{X_p\}_{p \neq j}$	Model score
CRT	Train	$\mathcal{F}(X_j \{X_p\}_{p \neq j})$	Yes	$X_j \perp\!\!\!\perp Y \{X_p\}_{p \neq j}$	LCD
GPF	Train Test	$\Phi(X_j)$	Yes	$X_j \perp\!\!\!\perp Y \{X_p\}_{p \neq j}$	LCD, Model score
Subset-GPF	Train Test	$\Phi(X_j)$	Yes	$X_j \perp\!\!\!\perp Y$	LCD, Model score

Subset-GPF is to reduce the computation costs of re-training experienced in CRT and Naive-GPF, by re-training on subsets \mathbf{Z} that are $N \times K$, instead of on the full design matrix \mathbf{X} , $N \times P$. Subset-GPF not only has computational advantages, but can avoid potential co-linearity problems, especially in datasets with $N \ll P$. The subsamples can mitigate confounding model contributions between highly correlated variables, by reducing the co-selection of correlated variables.

The hyperparameter K can be selected depending on the dataset and learning model. For models that learn covariance structures, which require K^2 observations, then let $K = \lceil \sqrt{N} \rceil$. Alternatively, K can be chosen to balance model needs and model computation speeds. A full discussion of the choice for K for various types of learning models, as well as the proof of the consistency of size K Subset-GPF, is provided in the Supplement.

3.2 GPF vs existing methods

Table 1 summarizes the properties of the various frameworks in terms of datasets perturbed, the perturbation function, and if the model f retrained after data perturbation. The last two columns spotlight, the null hypothesis and the test statistics. Note that for models that do not retrain, such as SHAP and HRT, the null is that a variable X_j is independent of Y given the pre-trained f and the other variables $X_{p \neq j}$.

4 Experiments

We first compare Subset-GPF (Algorithm 1) on synthetic datasets versus CRT and HRT, in terms of true positive rate (TPR), the false discovery rate (FDR) and the F_1 score. Then we apply GPF to a publicly available RNA expression dataset from the Allen Institute study on aging brains [25]. The experiments were run a combination of local CPU servers and AWS EC2 CPU servers.

4.1 Linear Gaussian data

Let \mathbf{X} be the design matrix of N observations of P variables, and \mathbf{y} the corresponding response vector. The dimensions were chosen with $N = 250$ and $P = 400$ to represent a sparse dataset. Moreover, let S denote the set of real explanatory variables with its size $|S| = 20$. Then \mathbf{X} and \mathbf{y} are generated as follows:

$$\mathbf{y} \sim \mathcal{N}(\beta \mathbf{X}, \sigma_y^2) \quad (1)$$

$$\mathbf{X} \sim \mathcal{N}(0, \Sigma_{\mathbf{x}}), \quad \beta_p = 0 \quad \text{if } X_p \notin S \quad (2)$$

$$\Sigma_{\mathbf{x}}^{ij} = \begin{cases} \sigma_x^2, & \text{if } i = j \\ \rho, & \text{if } i \neq j \end{cases} \quad (3)$$

To compare the performance of Subset-GPF, CRT and HRT on different signal to noise datasets, the dispersion of the variables and response were fixed, with $\sigma_x^2 = 1$ and $\sigma_y^2 = 1$. Moreover, the correlation was fixed $\rho = 0.3$, while β , was varied from $[0.5, 0.75, 1, 1.5, 2, 2.5, 3, 5, 7.5, 10]$. 5 datasets were generated from this data setup, and Subset-GPF, CRT and HRT were each run on each dataset using Lasso as the supervised learning model. Subset-GPF was run according to Algorithm 1, with $M = P$ for full coverage, $K = \lceil \sqrt{N} \rceil = 15$ and $R = 400$.

Similarly, to investigate the effect of correlated confounding variables, we let $\beta = 1$, $\sigma_x^2 = 1$ and $\sigma_y^2 = 1$, while ρ was varied from 0 to 0.9 in 0.1 increments. 5 datasets were generated from this data setup, and Subset-GPF, CRT and HRT were run on each dataset using Lasso as the training model.

4.2 Binomial transformed linear Gaussian data

The setup makes the following modification with the response \mathbf{y} now binary and are samples from the corresponding binomial distribution:

$$\mathbf{y} \sim \text{Bin}(1, \beta \mathbf{X}) \quad (4)$$

Just as in the linear Gaussian setup, 5 datasets with varying β were generated with all other parameters fixed. Then Subset-GPF and CRT run on each dataset now using Logistic Regression with a fixed L1 penalty as the training model. Next to investigate the confounding effect of correlated variables in this setup, β was fixed and ρ varied, and Subset-GPF and CRT run on the datasets generated from this condition.

4.3 Step-wise data

To investigate the performance of Subset-GPF on nonlinear models, we generated the response according to a step function:

$$\mathbf{z} \sim \mathcal{N}(\beta \mathbf{X}, 1) \quad (5)$$

$$y_i = \begin{cases} 1, & \text{if } z_i \in (\mathbf{z}_{25\%}, \mathbf{z}_{75\%}) \\ 0, & \text{otherwise} \end{cases}$$

The step-wise data can represent biological activations that are on ($y_i = 1$), when conditions are on in the middle of the range and off when conditions are in the tails. Subset-GPF and CRT were run on 5 datasets each for varying β and ρ for this step-wise setup, with the training model being XGBoost, a gradient boosted tree model [8].

4.4 Allen brain data experiments

The Allen Institute dataset on aging brains [25] consisted of 337 samples from 107 brains. The samples were collected from four areas in the brain: a) parietal cortex, b) temporal cortex, c) frontal white matter, and d) hippocampus. We used this publicly available gene-expression data with normalized fragments per kilobase of transcript per million (fpkm), corrected for batch and RNA quality using the RSEM pipeline [20]. The final number of genes in the normalized data was $P = 50281$. Consequently, the targets \mathbf{y} had $N = 337$ observations, each corresponding to one of four brain regions, and the variable matrix \mathbf{X} had dimensions 337×50281 . For the Allen brain data, Subset-GPF was applied to identify the genes that are significantly predictive of brain region under the XGBoost model.

5 Results

5.1 Synthetic data results

The Lasso coefficient difference (LCD) was the statistic used to determine which explanatory variables were not independent of the response for the linear Gaussian generated data for CRT and GPF, while HRT used the test MSE as its empirical risk. The TPR, positive predictive value ($\text{PPV} = 1 - \text{FDR}$), and F_1 are shown in Figure 1. The solid lines shows the mean, while the shaded areas correspond to the 95% CI determined by the 5 replication experiments.

When β is small, all frameworks miss some of the true explanatory variables, and TPR increases as β increases. In contrast, when the variable correlation ρ increases above 0.6, CRT and HRT struggle to find all true explanatory variables, while Subset-GPF still identifies nearly all. We note that this correlation setting is harder than in [7], which only considered auto-correlation, and not correlation across the entire variable set.

For the binomial transformed data, a modified LCD, as suggested in [7], was used as the statistic. Subset-GPF slightly outperformed CRT in terms of F_1 for all β and most ρ in Figure 2 a and b.

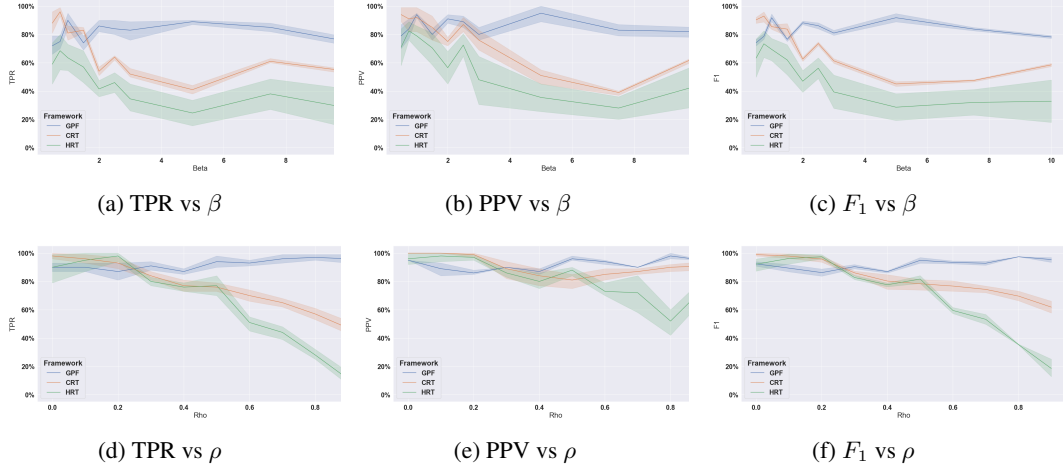


Figure 1: TPR, PPV and F_1 for GPF (blue), CRT (orange) and HRT (green) against signal strengths β in the top row, and against variable correlation ρ on bottom for the linear Gaussian data.

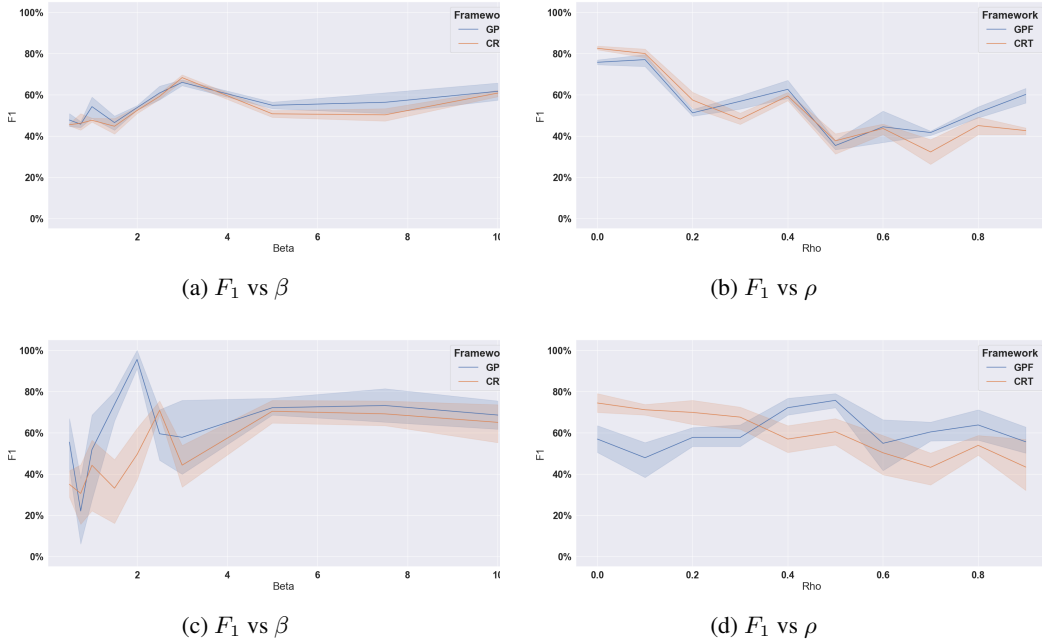


Figure 2: F_1 for CRT and GPF against signal strengths β in the left column, and against variable correlation ρ in the right with logistic data in the top row and step-wise data on the bottom.

Finally, for the step-wise data, the tree feature importance difference was used as the test statistic. The F_1 for Subset-GPF is slightly higher than CRT for various β and for the more challenging high correlation settings of ρ . We attempted to run HRT for the binomial and step-wise data, but was unsuccessful in determining significant different variables using the test accuracy as the HRT model score.

5.2 Complexity and run times

The training model complexities are shown in Table 2. Training the Lasso model is cubic in the number of variables D [10]. The logistic regression model, with no intercept C target classes, and maximum stopping epoch E , can be trained in $O(DCNE)$. For our experiments with logistic regression with L1 penalty, $E = 2000$. Finally, XGBoost takes $O(THDN \log N)$ [8], where T is the number and H the height of the trees. For our experiments using XGBoost, $T = 100$ and $H = 3$.

Table 2: Training Complexity

Model	$O(\cdot)$
Lasso	$O(D^3 + N \times D^2)$
Logistic	$O(D \times C \times N \times E)$
XGBoost	$O(T \times H \times D \times N \times \log N)$

Table 3: Run Times in seconds

Model	CRT	Subset-GPF
Lasso	1955 ± 81	229 ± 9
Logistic	10320 ± 448	772 ± 37
XGBoost	3277 ± 134	1300 ± 98

Since $D = P = 400$ for CRT, while $D = K = \lfloor \sqrt{N} \rfloor = 15$ for Subset-GPF in our synthetic data experiments, Subset-GPF is faster than CRT.

We measured running times for CRT and Subset-GPF for one variable X_1 clocked on the same CPU over 10 replications, and present them in Table 3. These training times include the conditional sampling for CRT and the random permutations for Subset-GPF.

As expected, Subset-GPF was substantially quicker to train for all three methods as it had lower number of variables $D = K = 15$, whereas CRT had to train over $D = P = 400$. We do note that training run times were not as different as the ratio of training complexity would suggest. This is partly due to an efficient conditional sampling based on the conditional multivariate Gaussian distribution implemented for CRT, while Subset-GPF used random shuffle permutations. These run times are for CRT or Subset-GPF on one variable, and would be expensive if all variables were run sequentially. Sequential run times can be reduced by parallelizing Subset-GPF and CRT in the cloud.

5.3 Allen Brain data results

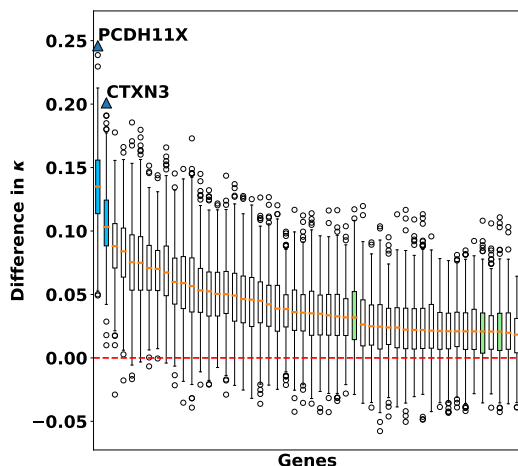


Figure 3: First 50 genes ordered by median $\Delta(\kappa_{\Phi_{x,\cdot}})$. Significant genes at $\alpha = \frac{0.05}{50000}$ are shaded blue. Green shaded boxes indicate randomly selected genes.

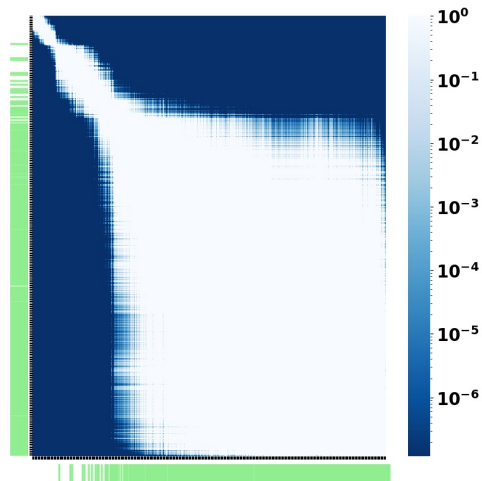


Figure 4: Pairwise Conover p-values of the ordered $\Delta(\kappa_{\Phi_{x,\cdot}})$ for all 500 genes. Green bars indicate randomly selected genes. Genes ordered in the same fashion as Figure 3 and C.1

We ran Subset-GPF (Algorithm 1) with f chosen to be XGBoost and $M = 500$ genes of interest, since we cannot run CRT or HRT as we do not know the marginal distribution of the genes. The genes of interest were chosen to be the top 100 genes in terms of feature importance from XGBoost, run on the entire variable matrix \mathbf{X} , and 400 randomly selected genes were chosen as well. Including the top 100 genes from XGBoost allowed us to analyze genes that would be expected to be in the tail distribution in terms of model contribution. The number of runs for each gene was set to be $R = 1000$. For each R , a subsample of $K - 1 = 49$ genes were used in combination with the tested gene x_{j_m} . In each run, the data was split randomly 80%-20% in terms of training and test. XGBoost was trained on the training portion and evaluated on the test. κ agreement were computed for test

predictions as this is a multi-class classification problem. Furthermore, the delta in κ on the test dataset for Subset-GPF was used as the test statistic.

Figure 3 shows the ordered differenced κ null distributions $\Delta(\kappa_{\Phi_x, \cdot})$, for 50 genes from Subset-GPF; the entire 500 gene plot is given in Supplemental Figure C.1. Two genes, *PCDH11X* and *CTXN3*, showed statistically significant effects after Bonferroni correction. We note that a few randomly selected genes, shaded green, were among the top 50 genes by $\Delta(\kappa_{\Phi_x, \cdot})$, suggesting that tail distribution of the top 100 genes is similar to random genes.

The Conover test with Bonferroni adjustment [9] was used to test differences in the differenced null distributions $\Delta(\kappa_{\Phi_x, \cdot})$ between every pairwise gene combination for all 500 genes (Figure 4). A small cluster of 14 genes (upper left) were found to be statistically indistinguishable from *PCDH11X* and *CTXN3* and were a XGBoost model was trained only on these genes to evaluate their sufficiency. For reference, XGBoost was run on these 14 genes without permutation, and achieved $\kappa = 0.85$, weighted $F1 = 0.89$ and $recall = 0.89$. These metrics shows that the 14 genes were sufficient for classification.

The three genes, *PCDH11x*, *CTXN3*, and *BHLHE22*, have been shown to be differentially expressed in targeted assays in the medical literature, but to our knowledge, not before in whole transcriptomic data. *PCDH11X* has been shown both by real-time reverse transcription-polymerase chain reaction amplification assays [5, 1] and by immunohistochemistry [28] to be differentially expressed in adult human brains. Wang et al. [39] showed that *CTXN3* is highly conserved among vertebrates with brain-specific expression. In *BHLB5* $-/-$ mice, [30] showed agency of the hippocampal commissure, anterior commissure, and corpus callosum. In addition, *BHLB5* has been shown to be a post-mitotic regulator of the neocortex including the frontal lobe. [16, 3] Interestingly, variants in both *PCDH11X* and *CTXN3* have been associated with schizophrenia [19, 26, 27, 33]. As a baseline comparison of another permutation framework, multiclass SAMseq [21] was run on the same dataset using 1000 permutations. No genes were found to be statistically significant with the default false discovery rate of 20% (Figure C.2).

6 Conclusion

We presented a generalized permutation framework, GPF, that is able to test for the significance of variables and their interactions in supervised models. The framework was applied to synthetic datasets and a high dimensional, real-world RNA expression dataset. Using GPF, we were able to identify significant variable interactions in a model-independent fashion for the synthetic datasets. In addition, we found genes in whole transcriptome data to be differentially expressed by brain regions. These genes have been previously confirmed in targeted biochemical and immunohistochemical assays to be differentially enriched across brain regions. Our experiments show promising results for the applicability of GPF in high-dimensional datasets with supervised models and its ability to elucidate statistical relationships among the variables.

References

- [1] Kung Ahn, Jae-Won Huh, Dae-Soo Kim, Hong-Seok Ha, Yun-Ji Kim, Ja-Rang Lee, and Heui-Soo Kim. Quantitative analysis of alternative transcripts of human PCDH11X/Y genes. *Am. J. Med. Genet. B Neuropsychiatr. Genet.*, 153B(3):736–744, April 2010.
- [2] André Altmann, Laura Tološi, Oliver Sander, and Thomas Lengauer. Permutation importance: a corrected feature importance measure. *Bioinformatics*, 26(10):1340–1347, 2010.
- [3] Francesco Bedogni, Rebecca D Hodge, Gina E Elsen, Branden R Nelson, Ray A M Daza, Richard P Beyer, Theo K Bammler, John L R Rubenstein, and Robert F Hevner. Tbr1 regulates regional and laminar identity of postmitotic neurons in developing neocortex. *Proc. Natl. Acad. Sci. U. S. A.*, 107(29):13129–13134, July 2010.
- [4] Thomas B Berrett, Yi Wang, Rina Foygel Barber, and Richard J Samworth. The conditional permutation test for independence while controlling for confounders. *Journal of the Royal Statistical Society: Series B (Statistical Methodology)*, 82(1):175–197, 2020.
- [5] P Blanco, C A Sargent, C A Boucher, M Mitchell, and N A Affara. Conservation of PCDHX in mammals; expression of human X/Y genes predominantly in brain. *Mamm. Genome*, 11(10): 906–914, October 2000.

- [6] Leo Breiman, Jerome H Friedman, Richard A Olshen, and Charles J Stone. *Classification and regression trees*. Routledge, 2017.
- [7] Emmanuel Candes, Yingying Fan, Lucas Janson, and Jinchi Lv. Panning for gold: ‘model-x’ knockoffs for high dimensional controlled variable selection. *Journal of the Royal Statistical Society: Series B (Statistical Methodology)*, 80(3):551–577, 2018.
- [8] Tianqi Chen and Carlos Guestrin. Xgboost: A scalable tree boosting system. In *Proceedings of the 22nd acm sigkdd international conference on knowledge discovery and data mining*, pages 785–794, 2016.
- [9] William Jay Conover and Ronald L Iman. On multiple-comparisons procedures. *Los Alamos Sci. Lab. Tech. Rep. LA-7677-MS*, pages 1–14, 1979.
- [10] Bradley Efron, Trevor Hastie, Iain Johnstone, and Robert Tibshirani. Least angle regression. 2004.
- [11] Ronald A Fisher. The design of experiments. 1949.
- [12] Polina Golland and Bruce Fischl. Permutation tests for classification: towards statistical significance in image-based studies. In *Biennial international conference on information processing in medical imaging*, pages 330–341. Springer, 2003.
- [13] Phillip Good. *Permutation tests: a practical guide to resampling methods for testing hypotheses*. Springer Science & Business Media, 2013.
- [14] Ian Goodfellow, Yoshua Bengio, and Aaron Courville. *Deep learning*. MIT press, 2016.
- [15] Wassily Hoeffding. The large-sample power of tests based on permutations of observations. *The Annals of Mathematical Statistics*, pages 169–192, 1952.
- [16] Pushkar S Joshi, Bradley J Molyneaux, Liang Feng, Xiaoling Xie, Jeffrey D Macklis, and Lin Gan. Bhlhb5 regulates the postmitotic acquisition of area identities in layers II-V of the developing neocortex. *Neuron*, 60(2):258–272, October 2008.
- [17] I Elizabeth Kumar, Suresh Venkatasubramanian, Carlos Scheidegger, and Sorelle Friedler. Problems with shapley-value-based explanations as feature importance measures. In *International Conference on Machine Learning*, pages 5491–5500. PMLR, 2020.
- [18] Robert Lehr. Sixteen s-squared over d-squared: A relation for crude sample size estimates. *Statistics in medicine*, 11(8):1099–1102, 1992.
- [19] Anastasia Levchenko, Stepan Davtian, Natalia Petrova, and Yegor Malashichev. Sequencing of five left-right cerebral asymmetry genes in a cohort of schizophrenia and schizotypal disorder patients from russia. *Psychiatr. Genet.*, 24(2):75–80, April 2014.
- [20] Bo Li and Colin N Dewey. Rsem: accurate transcript quantification from rna-seq data with or without a reference genome. *BMC bioinformatics*, 12(1):323, 2011.
- [21] Jun Li and Robert Tibshirani. Finding consistent patterns: a nonparametric approach for identifying differential expression in rna-seq data. *Statistical methods in medical research*, 22(5):519–536, 2013.
- [22] Fredrik Lindgren, Björn Hansen, Walter Karcher, Michael Sjöström, and Lennart Eriksson. Model validation by permutation tests: applications to variable selection. *Journal of Chemometrics*, 10(5-6):521–532, 1996.
- [23] Michael I Love, Wolfgang Huber, and Simon Anders. Moderated estimation of fold change and dispersion for rna-seq data with deseq2. *Genome biology*, 15(12):550, 2014.
- [24] Scott M Lundberg and Su-In Lee. A unified approach to interpreting model predictions. In *Advances in neural information processing systems*, pages 4765–4774, 2017.
- [25] Jeremy A Miller, Angela Guillozet-Bongaarts, Laura E Gibbons, Nadia Postupna, Anne Renz, Allison E Beller, Susan M Sunkin, Lydia Ng, Shannon E Rose, Kimberly A Smith, et al. Neuropathological and transcriptomic characteristics of the aged brain. *Elife*, 6:e31126, 2017.
- [26] Benjaporn Panichareon, Kazuhiro Nakayama, Sadahiko Iwamoto, Wanpen Thurakitwannakarn, and Wasana Sukhumsirichart. Association of CTXN3-SLC12A2 polymorphisms and schizophrenia in a thai population. *Behav. Brain Funct.*, 8:27, May 2012.

- [27] Steven G Potkin, Jessica A Turner, Guia Guffanti, Anita Lakatos, James H Fallon, Dana D Nguyen, Daniel Mathalon, Judith Ford, John Lauriello, Fabio Macciardi, and FBIRN. A genome-wide association study of schizophrenia using brain activation as a quantitative phenotype. *Schizophr. Bull.*, 35(1):96–108, January 2009.
- [28] Thomas H Priddle and Tim J Crow. Protocadherin 11X/Y a human-specific gene pair: an immunohistochemical survey of fetal and adult brains. *Cereb. Cortex*, 23(8):1933–1941, August 2013.
- [29] Marco Tulio Ribeiro, Sameer Singh, and Carlos Guestrin. " why should i trust you?" explaining the predictions of any classifier. In *Proceedings of the 22nd ACM SIGKDD international conference on knowledge discovery and data mining*, pages 1135–1144, 2016.
- [30] Sarah E Ross, Alejandra E McCord, Cynthia Jung, Denize Atan, Stephanie I Mok, Martin Hemberg, Tae-Kyung Kim, John Salogiannis, Linda Hu, Sonia Cohen, Yingxi Lin, Dana Harrar, Roderick R McInnes, and Michael E Greenberg. Bhlhb5 and prdm8 form a repressor complex involved in neuronal circuit assembly. *Neuron*, 73(2):292–303, January 2012.
- [31] Henry Scheffe. Statistical inference in the non-parametric case. *The Annals of Mathematical Statistics*, 14(4):305–332, 1943.
- [32] Ramprasaath R Selvaraju, Michael Cogswell, Abhishek Das, Ramakrishna Vedantam, Devi Parikh, and Dhruv Batra. Grad-cam: Visual explanations from deep networks via gradient-based localization. In *Proceedings of the IEEE international conference on computer vision*, pages 618–626, 2017.
- [33] Omar Šerý, Jan Lochman, Jana Povářová, Vladimír Janout, Jiří Plesník, and Vladimír J Balcar. Association between 5q23.2-located polymorphism of CTXN3 gene (cortexin 3) and schizophrenia in European-Caucasian males; implications for the aetiology of schizophrenia. *Behav. Brain Funct.*, 11:10, March 2015.
- [34] Karen Simonyan, Andrea Vedaldi, and Andrew Zisserman. Deep inside convolutional networks: Visualising image classification models and saliency maps. *arXiv preprint arXiv:1312.6034*, 2013.
- [35] Carolin Strobl, Anne-Laure Boulesteix, Thomas Kneib, Thomas Augustin, and Achim Zeileis. Conditional variable importance for random forests. *BMC bioinformatics*, 9(1):307, 2008.
- [36] Wesley Tansey, Victor Veitch, Haoran Zhang, Raul Rabadan, and David M Blei. The holdout randomization test for feature selection in black box models. *Journal of Computational and Graphical Statistics*, 31(1):151–162, 2022.
- [37] Gerald Van Belle. *Statistical rules of thumb*, volume 699. John Wiley & Sons, 2011.
- [38] Abraham Wald and Jacob Wolfowitz. Statistical tests based on permutations of the observations. *The Annals of Mathematical Statistics*, 15(4):358–372, 1944.
- [39] Hai Tao Wang, Ji Wu Chang, Zhi Guo, and Bao Guo Li. In silico-initiated cloning and molecular characterization of cortexin 3, a novel human gene specifically expressed in the kidney and brain, and well conserved in vertebrates. *Int. J. Mol. Med.*, 20(4):501–510, October 2007.
- [40] Brian D Williamson, Peter B Gilbert, Noah Simon, and Marco Carone. Nonparametric variable importance assessment using machine learning techniques. 2017.

A Conditional Randomization Test Algorithm

Algorithm A1 Conditional Randomization Test

- 1: **Input:** response $\mathbf{y} = \{y_i\}_{i=1}^N$, variables $\mathbf{X} = \{x_{ij}\}_{i=1, j=1}^{N, P}$, the marginal distribution $\mathcal{F}(\mathbf{X})$, a supervised model f , and feature importance statistic $T_j(\mathbf{X}, \mathbf{y})$
- 2: **for** $r = 1$ to R **do do**
- 3: **for** $j = 1$ to P **do do**
- 4: Sample

$$X_{ij}^{(r)} \sim \mathcal{F}(X_{ij} | \{X_{ip}\}_{p \neq j}), \forall i = 1, \dots, N \quad (6)$$

- 5: Replace column j in \mathbf{X} with $X_j^{(r)}$ to get $\mathbf{X}^{(r)}$
- 6: Compute $\mathbb{1}(T_j(\mathbf{X}^{(r)}, \mathbf{y}) \leq T_j(\mathbf{X}, \mathbf{y}))$
- 7: **end for**
- 8: **end for**
- 9: **Output:** One-sided p-values for $j = 1, \dots, P$:

$$p_j = \frac{1}{R+1} \left[1 + \sum_{r=1}^R \mathbb{1}(T_j(\mathbf{X}^{(r)}, \mathbf{y}) \leq T_j(\mathbf{X}, \mathbf{y})) \right] \quad (7)$$

In Candès et al. [7], the authors propose using coefficient of variable X_j from a fitted Lasso model f , with a penalty λ for linear-Gaussian datasets as the test statistic, so that $T_j(\mathbf{X}, \mathbf{y}) = \hat{b}_j(\lambda)$. Then the one-sided p-value test in Equation 7 simplifies to:

$$W_j^{(r)} = |\hat{b}_j(\lambda)| - |\hat{b}_j^{(r)}(\lambda)| \quad (8)$$

$$p_j = 1 - \frac{1}{R+1} \left[1 + \sum_{r=1}^R \mathbb{1}(W_j^{(r)} > 0) \right] \quad (9)$$

Here $\hat{b}_j^{(r)}(\lambda)$ denotes the coefficient of the perturbed variable $x_j^{(r)}$ in a fitted Lasso model with a penalty λ . Candès et al. [7] refers to Equation 9 as the Lasso Coefficient Difference (LCD). The intuition is that if variable X_j contributes to predicting \mathbf{y} under a linear model f , then its coefficient, $\hat{b}_j(\lambda)$, will be nonzero and larger than the coefficient, $\hat{b}_j^{(r)}(\lambda)$, of its perturbed version $X_j^{(r)}$.

B Naive GPF

A naive implementation of the full generalized permutation framework (Naive-GPF) incorporates these permutations and is shown in Algorithm A2. If T can be affected by stochasticity or different initial starting points of f , then Algorithm A2 line A2 can be moved inside the R loop, so that the same random seeds or initialization are used for each $r \in R$.

We note that the statistic T can be computed on either the training data or the test data. If T is computed on the training data, then Naive-GPF is similar to the CRT setup. If T is computed on the test data, then Naive-GPF is similar to the HRT setup. Specifically, for linear-Gaussian and logistic synthetic data, we adopted LCD as the statistic T for the training data. For the step-wise data, we used the feature importance of the XGBoost model as the statistic T on the training data. Let $\Delta(T_{\Phi_x, j})$ denote the differenced null distribution for variable j under Φ_x (10), then the one-sided p-value is given by Equation (11), where $\mathbb{1}$ is the indicator function. A one-sided test is used as we are only concerned with cases where the permuted data did not underperform, $T - T_{\Phi_x, j}^{(r)} > 0$.

$$\Delta(T_{\Phi_x, j}) = T - \{T_{\Phi_x, j}^{(r)}\}_{r=1}^R \quad (10)$$

$$p_j = \frac{1}{R+1} \left[1 + \sum_{r=1}^R \mathbb{1}(T - T_{\Phi_x, j}^{(r)} > 0) \right] \quad (11)$$

Algorithm A2 Permutation plug-in estimate for Naive-GPF

- 1: **Input:** response $\mathbf{y} = \{y_i\}_{i=1}^N$, variables $\mathbf{X} = \{x_{ij}\}_{i=1, j=1}^{N, P}$, and a supervised learning model f
 - 2: Sample training indices $\{\tau\}_{0 < \tau \leq N}$, with test indices being the remainder $\{1, \dots, N\} \setminus \{\tau\}$.
 - 3: Split \mathbf{y} and \mathbf{X} according to the training and test using A2.
 - 4: Train f on the training data $\{y_i, \{x_{ij}\}_{j=1}^P\}_{i \in \{\tau\}}$, and compute statistic T on the appropriate dataset.
 - 5: **for** $\phi \in [\Phi_y, \Phi_x]$ **do**
 - 6: **for** $r = 1$ **to** R **do**
 - 7: **if** $\phi == \Phi_y$ **then**
 - 8: Permute the labels, $\mathbf{y}'^{(r)} = \Phi_y(\mathbf{y})$
 - 9: Train f on $\{y'_i{}^{(r)}, \{x_{ij}\}_{j=1}^P\}_{i \in \{\tau\}}$, and compute the permuted data statistic $T_{\Phi_y}^{(r)}$
 - 10: **else**
 - 11: **for** $p = 1$ **to** P **do**
 - 12: Permute variable p , $\mathbf{x}'_{:,p}{}^{(r)} = \phi(\mathbf{x}_{:,p})$, so that $\mathbf{X}'^{(r)} = \{\mathbf{x}_{:,1}, \dots, \mathbf{x}'_{:,p}{}^{(r)}, \dots, \mathbf{x}_{:,P}\}$
 - 13: Train f on $\{y_i, \mathbf{x}'_i{}^{(r)}\}_{i \in \{\tau\}}$, and compute the permuted data statistic $T_{\phi,p}^{(r)}$
 - 14: **end for**
 - 15: **end if**
 - 16: **end for**
 - 17: **end for**
 - 18: **Output:** test statistic distributions $T, \{T_{\Phi_y}^{(r)}\}_{r=1}^R, \{\{T_{\Phi_x,j}^{(r)}\}_{r=1}^R\}_{j=1}^P$
-

B.1 Permutation interpretations

The first permutation Φ_y is the common label permutation, but applied to a supervised model f . The null hypothesis is that f does not learn a statistic T significantly different from the null distribution when the labels are scrambled and nothing should be learnable. This is in the spirit of SAMseq (Algorithm A4) [21], but applied to a supervised model f , whereas Algorithm A4 has $\{f_j\}_{j=1}^P$ models, where each f_j is the binary classification function applied to a variable $\mathbf{x}_{:,j}$. If the p-value from Equation (11) for $\Delta(T_{\Phi_y})$ is not significant, then model f is not predictive, and further permutation tests on variables with Φ_x will not be informative and are not needed.

The second permutation Φ_x constructs a null distribution on the effect of a variable of interest $\mathbf{x}_{:,j}$ in f .

B.2 Proof of subset-GPF consistency

The output of Subset-GPF, Algorithm 1, are the statistics $\{\{T_{j_m}^{(r)}\}_{r=1}^R\}_{m=1}^M$ and $\{\{T_{j_m}'^{(r)}\}_{r=1}^R\}_{m=1}^M$ for the variables $\{\mathbf{x}_{:,j_m}\}_{m=1}^M$ unpermuted and permuted, respectively. Since these statistics are paired given how X_{sub} are randomly sampled for each $\mathbf{x}_{:,j_m}$ and each r , they can be re-written for a given variable $\mathbf{x}_{:,j_m}$ as:

$$\{T_{j_m}^{(r)} - T_{j_m}'^{(r)}\}_{r=1}^R \quad (12)$$

Equation 12 has a similar form to the differenced null distribution for permutation ϕ and variable j from Algorithm A2 given in Equation 10, which can be re-written as:

$$\Delta(T_{\phi,j}) = \{T - T_{\phi,j}'^{(r)}\}_{r=1}^R \quad (13)$$

Furthermore, if f is affected by stochasticity or initial starting points, then Algorithm A2 line A2 can be moved inside the R loop, so that the same random seeds or initialization are used for each $r \in R$. In this case the statistic T in Equation 13 becomes:

$$\Delta(T_{\phi,j}) = \{T^{(r)} - T_{\phi,j}'^{(r)}\}_{r=1}^R \quad (14)$$

The main difference between Equations 12 and 14 is the underlying covariate matrix over which the statistic T is calculated. In Equation 14, the entire covariate matrix \mathbf{X} , with dimension $N \times P$, is

used:

$$T^{(r)} = T(\mathbf{y}, f(\mathbf{X})), \quad (15)$$

$$\text{and } T'_{\phi,j}{}^{(r)} = T(\mathbf{y}, f(\mathbf{X}')), \quad (16)$$

$$\text{where } \mathbf{X}' = [\mathbf{x}_{\cdot,1}, \dots, \phi(\mathbf{x}_{\cdot,j}), \dots, \mathbf{x}_{\cdot,P}] \quad (17)$$

In contrast in Equation 12, a $N \times K$ subsampled matrix \mathbf{Z} is used to compute T per Algorithm 1. Since \mathbf{Z} is sampled for every $r \in R$ for variable \mathbf{x}_{\cdot,j_m} , it can be expressed more precisely as $\mathbf{Z}_{j_m}^{(r)} = [\mathbf{x}_{\cdot,j_m}, \mathbf{X}_{sub}^{(r)}]$, so that:

$$T_{j_m}^{(r)} = T(\mathbf{y}, f(\mathbf{Z}_{j_m}^{(r)})), \quad (18)$$

$$\text{and } T'_{j_m}{}^{(r)} = T(\mathbf{y}, f(\mathbf{Z}'_{j_m}{}^{(r)})), \quad (19)$$

$$\text{where } \mathbf{Z}'_{j_m}{}^{(r)} = [\Phi_x(\mathbf{x}_{\cdot,j_m}), \mathbf{X}_{sub}^{(r)}] \quad (20)$$

Then $\{\mathbf{Z}_{j_m}^{(r)}\}_{r=1}^R = [\mathbf{x}_{\cdot,j_m}, \mathbf{X}_{sub}^{(r)}]_{r=1}^R$ are the R sampled $N \times K$ matrices that include \mathbf{x}_{\cdot,j_m} , and $\{T_{j_m}^{(r)}\}_{r=1}^R$ the corresponding statistics. Let $\bar{T}_{j_m} = \frac{1}{R} \sum_{r=1}^R T_{j_m}^{(r)}$, then by the Law of Large Numbers:

$$\bar{T}_{j_m} \rightarrow \mu_{j_m} \quad \text{for } R \rightarrow \infty \quad (21)$$

where μ_{j_m} is the mean of T for random $N \times K$ subsamples of \mathbf{X} that include \mathbf{x}_{\cdot,j_m} . Equation 21 is intuitive since $\lim_{R \rightarrow \infty} \{T_{j_m}^{(r)}\}_{r=1}^R$ is the sampling distribution of T_{j_m} .

Now consider the case for \mathbf{x}_{\cdot,j_m} permuted, so that $\{\mathbf{Z}'_{j_m}{}^{(r)}\}_{r=1}^R = [\Phi_x(\mathbf{x}_{\cdot,j_m}), \mathbf{X}_{sub}^{(r)}]_{r=1}^R$. Since there are a finite $N!$ permutations of $\mathbf{x}_{\cdot,j_m} = \{x_{ij}\}_{i=1}^N$, and the permutations are independent of the subsampling of $\mathbf{X}_{sub}^{(r)}$ from \mathbf{X} , the corresponding statistics $\{T'_{j_m}{}^{(r)}\}_{r=1}^R$ also converges as $R \rightarrow \infty$:

$$\bar{T}'_{j_m} = \frac{1}{R} \sum_{r=1}^R T'_{j_m}{}^{(r)} \quad (22)$$

$$\bar{T}'_{j_m} \rightarrow \mu'_{j_m} \quad \text{for } R \rightarrow \infty \quad (23)$$

where μ'_{j_m} is the mean of T' for $N \times K$ subsamples of \mathbf{X} that include $\Phi_x(\mathbf{x}_{\cdot,j_m})$. This means that the sampled distribution of differenced statistics $\{T_{j_m}^{(r)} - T'_{j_m}{}^{(r)}\}_{r=1}^R$ converges to the differenced null distribution for K subsampled variables from \mathbf{X} that contain \mathbf{x}_{\cdot,j_m} , and Subset-GPF (Algorithm 1) yields samples from the desired null distribution.

B.3 Calibration of subsample size K

The subsample size K for Subset-GPF can be calibrated in two ways. First, we can balance the computational requirements of the learning model and Subset-GPF. For example, in models, such as linear and generalized linear models, that learn a covariance structure between the covariates, which require K^2 observations, let $K = \lfloor \sqrt{N} \rfloor$. Next consider R , the number of subsamples to run in Subset-GPF. The number of all subsets of size K is $\binom{P}{K}$, and is generally too large to be computationally feasible. A more computationally feasible choice of $R = \left(\frac{P}{K}\right)^2$, provides an adequate mix of subset samples for each variable of interest. This method yields the following computational cost for Subset-GPF, derived by taking the model training complexities in Table 2, multiplying by the number of runs R , and substituting $R = \left(\frac{P}{K}\right)^2$.

The second way to choose the subsample size K is given by the desired goal of Subset-GPF (Algorithm 1), which is to identify variables that significantly affect model predictive performance, by relating the subsample size to the model performance metric T . This is done through Algorithm A3. We can use a range around $K = \lfloor \sqrt{N} \rfloor$ for K_0 and K_1 . The intuition is to find a $K_0 \leq k \leq K_1$, where model f is significantly predictive of T on subsamples \mathbf{Z} compared to the label scrambled null

Table 4: Subset-GPF Complexity

MODEL UNDER SUBSET-GPF	$O(\cdot)$
LASSO	$O(K^3 + N \times K^2) \times (\frac{P}{K})^2 = O(K + N)P^2$
LOGISTIC REGRESSION	$O(K \times C \times N \times E) \times (\frac{P}{K})^2 = O(\frac{P^2}{K}CNE)$
XGBOOST	$O(T \times H \times K \times N \times \log N) \times (\frac{P}{K})^2 = O(\frac{P^2}{K}THN \log N)$

Algorithm A3 Calibrating subsample size K

- 1: **Input:** labels $\mathbf{y} = \{y_i\}_{i=1}^N$, covariates $\mathbf{X} = \{x_{ij}\}_{i=1, j=1}^{N, P}$, and supervised model f
- 2: **for** $k = K_0$ **to** K_1 **do**
- 3: **for** $r = 1$ **to** R **do**
- 4: Subsample $\mathbf{Z}_k^{(r)}$, dimension $N \times K$ from \mathbf{X} randomly.
- 5: Split \mathbf{y} and $\mathbf{Z}_k^{(r)}$ into training and test sets.
- 6: Train and compute the test statistic $T_k^{(r)}$ from \mathbf{y} , $\mathbf{Z}_k^{(r)}$ and f .
- 7: Permute the labels $\mathbf{y}'^{(r)} = \Phi_{\mathbf{y}}(\mathbf{y})$
- 8: Train and compute the test statistic $T_{\Phi_{\mathbf{y}}, k}^{(r)}$ from $\mathbf{y}'^{(r)}$, $\mathbf{Z}_k^{(r)}$ and f .
- 9: **end for**
- 10: **end for**
- 11: **Output:** $\{\{T_{\Phi_{\mathbf{y}}, k}^{(r)}\}_{r=1}^R\}_{k=K_0}^{K_1}$, the null distribution of $\{\{T_k^{(r)}\}_{r=1}^R\}_{k=K_0}^{K_1}$

distribution (25).

$$\Delta(T_{\Phi_{\mathbf{y}}, k}) = \{T_k^{(r)} - T_{\Phi_{\mathbf{y}}, k}^{(r)}\}_{r=1}^R \quad (24)$$

$$\text{p-value} = \frac{1}{R} \sum_{r=1}^R I(T_k^{(r)} - T_{\Phi_{\mathbf{y}}, k}^{(r)} < 0) \quad (25)$$

Note the upper limit for K_1 is $K_1 = P$.

B.4 Calibrating the number of perturbations R in subset-GPF for a desired TPR level

We show how to calibrate the TPR or power of subset-GPF by choosing R for a given K for two major types of response and variable relationships. First, we consider linear-Gaussian relationships:

$$\mathbf{X} \sim \mathcal{N}(0, \text{diag}(\sigma_x^2)) \quad (26)$$

$$y_i = \sum_{j=1}^P \beta_j x_{ij} + \epsilon_i, \quad \text{where } \epsilon_i \sim \mathcal{N}(0, \sigma_y^2) \quad (27)$$

$$\mathbf{y} \sim \mathcal{N}(\beta \mathbf{X}, \sigma_y^2) \quad (28)$$

For this setup, the coefficients for the linear model f are estimated as:

$$\hat{\beta} = (\mathbf{X}^\top \mathbf{X})^{-1} \mathbf{X}^\top \mathbf{y} \quad (29)$$

$$\beta \sim \mathcal{N}(\hat{\beta}, (\mathbf{X}^\top \mathbf{X})^{-1} \sigma_y^2) \quad (30)$$

The coefficient for the unperturbed variable x_j is $\hat{\beta}_j$. In the full naive-GPF, the variable x_j is permuted to become $x_j^{(r)} = \Phi_x(x_j)$, and the estimate of the coefficient becomes:

$$\mathbf{X}'^{(r)} = \{\mathbf{x}_{\cdot, 1}, \dots, \mathbf{x}'_{\cdot, j}, \dots, \mathbf{x}_{\cdot, P}\} \quad (31)$$

$$\hat{\beta}' = (\mathbf{X}'^{(r)\top} \mathbf{X}'^{(r)})^{-1} \mathbf{X}'^{(r)\top} \mathbf{y} \quad (32)$$

Then the coefficient of the perturbed variable $x_j^{(r)}$ is $\hat{\beta}'_j$. One nuance is that the distribution of the β' depends on whether x_j is in the set of variables of real explanatory variables S :

$$\beta' \sim \begin{cases} \mathcal{N}(\hat{\beta}, (\mathbf{X}^\top \mathbf{X})^{-1} \sigma_y^2) & x_j \notin S \\ \mathcal{N}(\hat{\beta}', ((\mathbf{X}^\top \mathbf{X})^{-1} \sigma_y^2 + (\beta_j x_j)^2)) & x_j \in S \end{cases} \quad (33)$$

If $x_j \in S$ and x_j is perturbed, then $\mathbf{y} - \beta\mathbf{X}' = \epsilon + \beta_j x_j$. That is the residual will be bigger by $\beta_j x_j$ even if the true linear weights β are used. This result can be easily verified by simulation.

The full GPF uses the LCD to test the significance of variable x_j : $\text{LCD}_j^{(r)} = |\hat{\beta}_j| - |\hat{\beta}'_j|$. Then for the LCD to have 90% TPR at $\alpha = 0.05$ from a 1-sided t-distribution, the number of perturbation simulations for variable x_j , assuming that x_j is in the set of explanatory variables S is given by the rule of thumb [18, 37]:

$$R = 11 \times \frac{\text{var}(\hat{\beta}')}{(\mathbb{E}(\text{LCD}))^2} \quad (34)$$

$$\mathbb{E}_r(\text{LCD}_j) = \mathbb{E}_r(|\hat{\beta}_j| - |\hat{\beta}'_j|) = |\hat{\beta}_j| = \beta_j \quad (35)$$

$$\text{var}(\hat{\beta}') = (\mathbf{X}^\top \mathbf{X})^{-1} \sigma_y^2 + (\beta_j x_j)^2 \quad (36)$$

$$\approx (N^2 \sigma_x^2)^{-1} \sigma_y^2 + (\beta_j \sigma_x)^2 \quad (37)$$

$$\implies R \approx 11 \times \frac{(\beta_j \sigma_x)^2}{\beta_j^2} \quad (38)$$

Now consider the case of subset-GPF, which subsamples $K - 1$ variables uniform randomly and combines them with a variable of interest x_j . The subset coefficient β_{sub} is given by:

$$\hat{\beta}_{sub} = (\mathbf{X}_{sub}^\top \mathbf{X}_{sub})^{-1} \mathbf{X}_{sub}^\top \mathbf{y} \quad (39)$$

$$\beta_{sub} \sim \mathcal{N} \left(\hat{\beta}_{sub}, \left((\mathbf{X}_{sub}^\top \mathbf{X}_{sub})^{-1} \sigma_y^2 + \left(\frac{P-K+1}{P-1} \times |S| \bar{\beta} \right)^2 \right) \right) \quad (40)$$

The $\frac{P-K+1}{P-1} \times |S| \bar{\beta}$ adjustment accounts for how many explanatory variables from S would not be included in uniformly randomly chosen subsamples of size $K - 1$ from the set of $P - 1$ variables not including x_j , with $\bar{\beta}$ the average weight of the explanatory variables. Next, if x_j is perturbed, the distribution of β'_{sub} is:

$$\hat{\beta}'_{sub} = (\mathbf{X}_{sub}^{(r)\top} \mathbf{X}_{sub}^{(r)})^{-1} \mathbf{X}_{sub}^{(r)\top} \mathbf{y} \quad (41)$$

and the distribution of β'_{sub} is:

$$\beta'_{sub} \sim \begin{cases} \mathcal{N} \left(\hat{\beta}_{sub}, \left((\mathbf{X}_{sub}^\top \mathbf{X}_{sub})^{-1} \sigma_y^2 + \left(\frac{P-K+1}{P-1} \times |S| \bar{\beta} \right)^2 \right) \right) & x_j \notin S \\ \mathcal{N} \left(\hat{\beta}'_{sub}, \left((\mathbf{X}_{sub}^\top \mathbf{X}_{sub})^{-1} \sigma_y^2 + \left(\frac{P-K+1}{P-1} \times |S| \bar{\beta} \right)^2 + (\beta_j x_j)^2 \right) \right) & x_j \in S \end{cases} \quad (42)$$

Then the subset-GPF LCD for x_j is $|\hat{\beta}_{j,sub}| - |\hat{\beta}'_{j,sub}|$. For this LCD to be powered at the 90% level or have 90% TPR with $\alpha = 0.05$, the number of runs R , based on the 1-sided t-distribution, should be: $R = 11 \times \frac{\text{var}(\hat{\beta}'_{sub})}{\mathbb{E}(\text{LCD})^2} \approx 11 \left(\frac{P-K}{P} \times |S| \bar{\beta} \right)^2 / \beta_j^2$. For our experiments on synthetic linear-Gaussian and logistic data, with $N = 250$, $P = 400$, $|S| = 20$, common β for variables in the explanatory variable set S , so that $\bar{\beta} = \beta_j$, and $K = \lfloor \sqrt{N} \rfloor = 15$, $R \approx 3970$ for 90% TPR. More generally, additive models that are not linear in x_j can be approximated by linear models by adding transformations of x_j to the design matrix \mathbf{X} . These added transformations will increase the variable dimension P to P' , and the R calibration calculation should be adjusted for P' .

Next, consider the class of models that are not additive, but links the response \mathbf{y} to a non-linear function of at least two explanatory variables. Suppose that when two or more explanatory variables included in training a model, the model learns and predicts held-out test responses \mathbf{t}_{est} with much lower MSE for real-valued \mathbf{y} or F1 score for categorical \mathbf{y} . Then in subset-GPF, we require that random samples of $K - 1$ variables contain at least one other explanatory variable with 90% probability to complement the variable being studied through permutation perturbations to detect significant differences in model performance. Therefore K can be chosen based on S or \hat{S} an estimate if S unknown so that K satisfies: $90\% = 1 - \left(\frac{P-S}{P} \right)^{K-1}$. This amounts to the shared birthday problem, and shows how we can effectively cover the space P variables with $R \binom{P}{K}$ subsamples.

Algorithm A4 Permutation plug-in estimate

- 1: **Input:** labels $\mathbf{y} = \{y_i\}_{i=1}^N$, covariates $\mathbf{X} = \{x_{ij}\}_{i=1, j=1}^{N, P}$. Let variable $\mathbf{x}_{\cdot, j} = \{x_{ij}\}_{i=1}^N$
 - 2: Compute the test statistics $\{T_j\}_{j=1}^P$ from \mathbf{y} for each variable $\mathbf{x}_{\cdot, j}$
 - 3: **for** $r = 1$ **to** R **do**
 - 4: Permute the labels \mathbf{y} to get $\mathbf{y}^{(r)}$
 - 5: Compute $\{T_j^{(r)}\}_{j=1}^P$ from the permuted labels $\mathbf{y}^{(r)}$ and unchanged variables $\{\mathbf{x}_{\cdot, j}\}_{j=1}^P$
 - 6: **end for**
 - 7: **Output:** $\{\{T_j^{(r)}\}_{r=1}^R\}_{j=1}^P$, the null distribution of $\{T_j\}_{j=1}^P$
-

C SAMseq algorithm

Li and Tibshirani [21] considered the case of N observations of $\{y_i\}_{i=1, \dots, N}$ belonging to one of two classes, C_1 or C_2 and N observations of P variables $\{x_{ij}\}_{i=1, \dots, N; j=1, \dots, P}$. The ranks of each variable x_j and the two-sample Wilcoxon statistic is used as T_j^k for each class:

$$R(X_{ij}) = \text{rank of } x_{ij} \text{ in } \{x_{ij}\}_{i=1, \dots, N} \quad (43)$$

$$T_j^k = \sum_{y_i \in C_k} R(X_{ij}) - \frac{|C_k|(N+1)}{2} \quad (44)$$

Note that the term $\frac{|C_k|(N+1)}{2}$ differs from the standard Wilcoxon rank statistic as it adjusts for class-imbalanced datasets through the class size $|C_k|$. The corresponding statistic for the r^{th} label permuted data is:

$$T_j^{k(r)} = \sum_{y_i^{(r)} \in C_k} R(X_{ij}) - \frac{|C_k|(N+1)}{2} \quad (45)$$

The p-value of each x_j is computed by comparing T_j^k to $T_j^{k(r)}$:

$$p_j^k = \frac{1}{R+1} \left[1 + \sum_{r=1}^R \mathbb{1}(|T_j^{k(r)}| \geq |T_j^k|) \right] \quad (46)$$

SAMseq estimates the probability a variable x_j is over or under-expressed for a class k by considering how likely the distribution of its ranksum would occur given random uniform permutations of the y class labels. As SAMseq only considers ranks of observed variables, it makes no distributional assumptions and is non-parametric. However, SAMseq can only detect over or under-expressed variables. It does not consider more complicated relationships between \mathbf{y} and \mathbf{X} through a model f . We note SAMseq could have been implemented by permuting the variables x_j while keeping \mathbf{y} unchanged and computing ranks on the permuted x_j . It was implemented by permuting \mathbf{y} because that breaks the relationship between the labels \mathbf{y} and all the variables \mathbf{X} and is more computationally efficient. However, if a more complicated functional model f is learnt between \mathbf{y} and \mathbf{X} , then one would want to ascertain the contribution of individual variables x_j to learning f given \mathbf{y} and all the other variables $\{x_i\}_{i \neq j}$. In this case, the x_j need to be permuted separately while the labels are kept unchanged. This is the approach adopted by GPF, CRT and HRT.

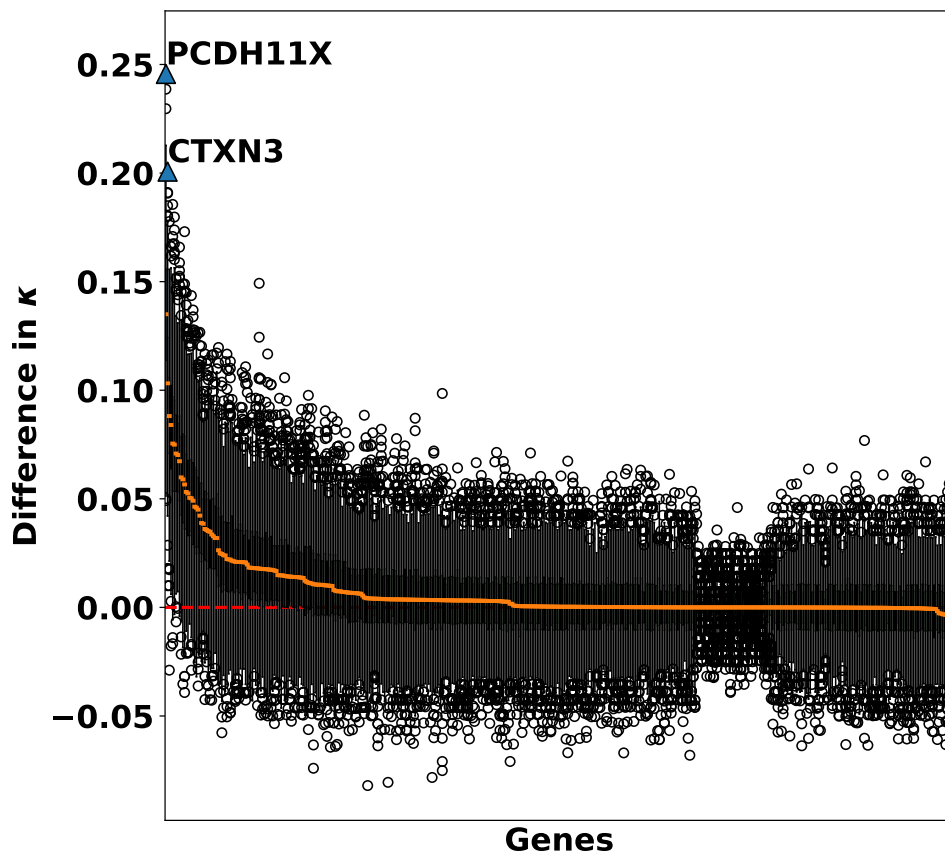


Figure C.1: $\Delta(\kappa)$ for the 500 genes. Green shaded boxes indicate randomly selected genes. Significant genes at $\alpha = \frac{0.05}{50000}$ are shaded blue and labeled.

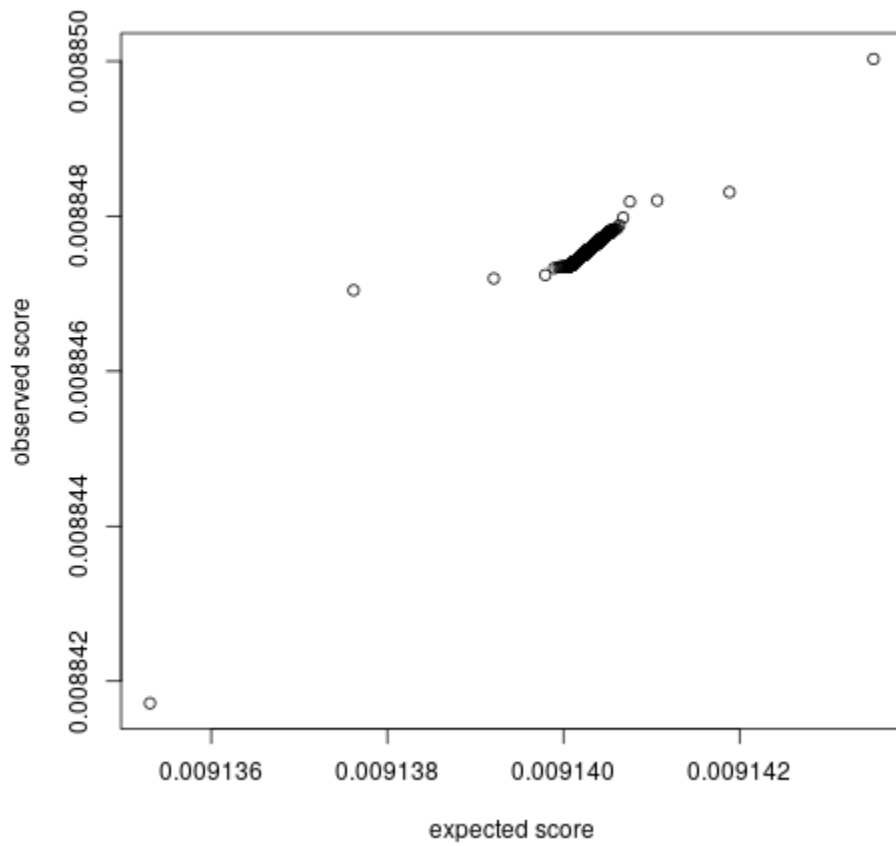


Figure C.2: Q-Q plot for SAMseq for multiclass prediction of brain region using the Allen brain gene-expression dataset. Of note, none of the genes are significantly different from the null distribution.